of the nature of the glassy state.

Acknowledgment. This work was supported in part by NSF Grant DMR 80-04236.

Appendix

A derivation of eq 6 is given here. The natural choice for the reference volume v, to be used in eq 4, would be a sphere, within which the form factor equals unity and without which it equals zero. The Fourier transform of such a form factor decays slowly with increasing s (approximately as s^{-4}). As a result the integral in eq 4, with $I(s)$ given by eq 5, diverges. The divergence can, of course, be avoided if we use a realistic $I(s)$ for larger s, since eq 5 obviously grossly overestimates the true scattered intensity at large s. An alternate, approximate method is to use a form factor that does not drop abruptly from unity to zero at its boundaries. We adopt the following form factor:

$$\sum(r) = 2^{3/2} \exp(-\tfrac{1}{2}r^2/\sigma^2) \tag{A1}$$

Its volume is given by

$$v = \int \sum(r)(4\pi r^2)\, dr = (2\pi^{1/2}\sigma)^3 \tag{A2}$$

and its Fourier transform by

$$\Phi(s) = (2\pi^{1/2}\sigma)^3 \exp(-2\pi^2\sigma^2 s^2) \tag{A3}$$

The normalization constant $2^{3/2}$ for $\sum(r)$ is given by the requirement that

$$(1/v)\int \Phi^2(s)(4\pi s^2)\, ds = 1$$

Substitution of (A3) and (5) into eq 4 then leads to eq 6 shown.

References and Notes

(1) Kovacs, A. J. *Fortschr. Hochpoly. Forsch.* **1963**, *3*, 394.
(2) Petrie, S. E. B. *J. Polym. Sci., Part A* **1972**, 1255.
(3) Struik, L. C. E. "Physical Aging in Amorphous Polymers and Other Materials"; Elsevier: Amsterdam, 1978.
(4) Guinier, A.; Fournet, G. "Small-Angle Scattering of X-rays"; Wiley: New York, 1955.
(5) Wendorff, J. H.; Fischer, E. W. *Kolloid Z. Z. Polym.* **1973**, *251*, 876, 884.
(6) Renninger, A. L.; Wicks, G. G.; Uhlmann, D. R. *J. Polym. Sci., Polym. Phys. Ed.* **1975**, *13*, 1247.
(7) Renninger, A. L.; Uhlmann, D. R. *J. Polym. Sci., Polym. Phys. Ed.* **1975**, *13*, 1481; **1976**, *14*, 415; **1978**, *16*, 2237.
(8) Straff, R. S.; Uhlmann, D. R. *J. Polym. Sci., Polym. Phys. Ed.* **1976**, *14*, 353.
(9) Matyi, R. J.; Uhlmann, D. R.; Koutsky, J. A. *J. Polym. Sci., Polym. Phys. Ed.* **1980**, *18*, 1053.
(10) Ruland, W. *Prog. Colloid Polym. Sci.* **1975**, *57*, 192.
(11) Rathje, J.; Ruland, W. *Colloid Polym. Sci.* **1976**, *254*, 358.
(12) Wiegand, W. Inaugural-Dissertation, Marburg/Lahn, 1977.
(13) Edwards, S. F. *Polymer* **1976**, *17*, 933. *Ann. N.Y. Acad. Sci.* **1981**, *371*, 210.
(14) Roe, R.-J., submitted for publication.
(15) Roe, R.-J.; Chang, J. C.; Fishkis, M.; Curro, J. J. *J. Appl. Crystallogr.* **1981**, *14*, 139.
(16) Kratky, O.; Pilz, I.; Schmitz, P. J. *J. Colloid Interface Sci.* **1966**, *21*, 24.
(17) Hellwege, K.-H.; Knappe, W.; Lehman, P. *Kolloid Z. Z. Polym.* **1962**, *183*, 110.
(18) Quach, A.; Simha, R. *J. Appl. Phys.* **1971**, *42*, 4592.
(19) Richardson, M. J.; Savill, N. G. *Polymer* **1977**, *18*, 3.
(20) Davies, R. O.; Jones, G. O. *Adv. Phys.* **1953**, *2*, 370.
(21) Roe, R.-J. *J. Appl. Phys.* **1977**, *48*, 4085.
(22) Robertson, R. E. *J. Polym. Sci., Polym. Symp.* **1978**, *No. 63*, 173.

Experimental Measurements of the Temporal Evolution of Cluster Size Distributions for High-Functionality Antigens Cross-Linked by Antibody

Gustav K. von Schulthess and George B. Benedek*

Department of Physics and Center for Materials Sciences and Engineering, Massachusetts Institute of Technology, Cambridge, Massachusetts 02139

Ralph W. De Blois

General Electric Research Laboratories, Schenectady, New York 12345.
Received May 25, 1982

ABSTRACT: Using a very sensitive Nanopar resistive pulse analyzer, we have been able to determine the temporal evolution of the cluster size distributions produced by bivalent antibodies cross-linking 0.235-μm polystyrene spheres coated with antigen. If X_n is the mole fraction of clusters containing n spheres and X_0 the mole fraction of spheres initially added, then it is found that the cluster size distributions are determined solely by the bonding parameter $b \equiv 1 - \sum X_n/X_0$. We report here the dependence of b upon the time t, the cross-linking antibody concentration $[ab]_0$, and X_0, the sphere concentration. We have compared these results for $b(t)$ and our previously reported form of the cluster size distribution $X_n/X_0 = (1-b)(be^{-b})^{n-1}/bn!$ with extant statistical and kinetic theories.

Introduction

The formation of a distribution of various size clusters through the interaction between initially distinct units is a central feature of widely diverse processes in chemistry, biology, and physics. Examples of these are polymerization processes in organic chemistry, antibody–antigen binding in immunology, coagulation processes in aerosol and colloidal physics, phase transitions in disordered magnetic spin systems, and percolation processes in statistical physics.

Two viewpoints have been taken to describe the temporal evolution of the cluster size distributions. In the first, the temporally evolving distributions are described by means of a set of coupled differential equations: the Smoluchowski equations,[1] whose coefficients, the bimolecular reaction rate coefficients $a_{nn'}$, depend upon the

0024-9297/83/2216-0434$01.50/0

number of units (n and n') in each pair of interacting clusters. These equations have been solved for a number of mathematical forms for the dependence of $a_{nn'}$ upon n and n'.[2-7] In the second point of view the distribution at each instant of time is assumed to be the one statistically most probably consistent with a given probability or degree of reaction α.[2,8] A recent review of equilibrium and kinetic theories of the cluster size distributions has been published.[9]

Despite the substantial theoretical literature there has been a lamentable paucity of experimental data on the form and temporal evolution of the cluster size distributions. This no doubt has been due to the experimental difficulties associated with the detection of clusters of small organic molecules in the case of polymerization reactions. We have recently reported[10] measurements of the form of the cluster size distributions for a condensing system that in the organic polymer notation contains units of the form RA_f and B_2. Here the RA_f unit contains f functional A units, each of which can bind to one of the two B sites on each B_2 unit. No AA or BB bonds can be formed. In our experiments the RA_f units are latex spheres (diameter 0.235 μm) covalently coated with the antigens human serum albumin (hSA), which act as the A sites. The B_2 units are complementary bivalent antibodies (goat anti human serum albumin). The size distributions were measured with a resistive pulse particle counter developed by De Blois and Bean.[11] This method when applied to the submicron condensing units had the following unique advantages. (1) Individual clusters could be studied without disturbing the reaction kinetics. (2) The high antigenic valency of the reacting units ($f \sim 10^3$) permits the use of very small concentrations of RA_f and B_2 units, with a consequent slow progression of the reaction.

Indeed, the time constants for the reaction were long, of the order of 100 min, while the time required to obtain an experimental histogram of the distribution was only about 3 min. As a result the experimentally obtained distributions can be regarded as essentially instantaneous in comparison with the time course of the reaction.

In our previous paper[10] it was found that the experimental cluster size distributions are functions of a single bonding parameter b and that the distribution is well represented by the expression

$$\frac{X_n}{X_0} = \frac{1-b}{b}(be^{-b})^n\frac{n^{n-1}}{n!} \tag{1}$$

Here X_n is the mole fraction of clusters, each of which contains n spheres. X_0 is the mole fraction of monomeric spheres initially placed in solution. b was obtained experimentally as

$$b = 1 - \frac{\sum_{n=1}^{\infty} X_n}{\sum_{n=1}^{\infty} nX_n} = 1 - \frac{\sum_{n=1}^{\infty} X_n}{X_0} = \frac{\sum_{1}^{\infty}(n-1)X_n}{X_0} \tag{2}$$

If the clusters are Cayley trees, i.e., if there are no cyclic structures, an n-mer contains $n-1$ bonds between spheres. Thus, b corresponds to the mean number of bridge-forming B_2 units in all the clusters per sphere initially added.

In this work we shall present a systematic investigation of the temporal evolution of the parameter b as a function of the concentration $[C_0]$ of latex spheres (RA_f units) and the concentration $[ab]_0$ of antibodies (B_2 units) initially placed in solution. The information presented here and in the previous papers[10,12] taken together characterizes the kinetic evolution of this RA_f-B_2 system and serves as a means of testing the basic statistical and kinetic theories.[2-9]

Materials and Methods

(a) Materials. Carboxylated Dow latex spheres of 0.235-μm diameter, to which human serum albumin (hSA) had been coupled covalently by a carbodiimide reaction, were kindly provided by Dr. Hans Hager of the Hoffmann-La Roche Co., Nutley, NJ. The stock solution provided was processed to remove latex sphere aggregates present prior to the addition of antibody. This was done by the method described previously.[10] It resulted in a decrease of the nonspecific aggregates from ~25% to less than 3% by weight. The latex sphere concentration in the processed solution was determined by dry weighing as well as by the use of the resistive pulse method.[10]

Antiserum containing anti-hSA antibody at a concentration of 9.6 mg/mL, as determined by precipitin analysis, was also kindly provided by Dr. Hager. Appropriate dilutions of this antibody were used as the combining agent in our studies after filtration through 0.2-μm Nucleopore filters obtained from Nuclepore Corp. The aggregation experiments were performed at room temperature (24 ± 2 °C) using as a diluent 0.1 M Tris buffer at pH 8.15. The corresponding ionic strength of the medium produced a Debye shielding length of approximately 0.5 nm. Various dilutions of latex spheres were incubated with various dilutions of antibody promptly after dilution of the latter, thus initiating the aggregation process. The specificity of the reaction was checked by incubating hSA latex spheres with rabbit anti human chorionic gonadotropin (hCG) antibody and alternatively by incubating hCG-coated latex spheres with hSA antibody. In both cases no aggregation was observed for the latex sphere and antibody concentrations of interest for a period of up to 3 days. This was the maximum period of observation for all the samples studied in this work.

(b) Method. The distribution of cluster sizes was measured with a resistive pulse analyzer.[10,11] In our case, the experimental setup consisted of two 1-mL chambers separated by a polycarbonate film of about 8-μm thickness that contained a single ~2-μm-diameter pore. A pressure head of 10 cm H_2O produces a flux of latex sphere aggregates across the pore. A constant-current source produces ~1.8 V across the pore. This served to measure the change in pore resistivity that is produced when an insulating latex sphere cluster as well as the ionic conducting solution medium passes through the pore. For clusters with linear dimensions smaller than ~$^1/_2$ the pore diameter there exists a linear relationship between the change in the voltage across the pore and the volume of the cluster in the pore. By accumulating the number of pulses in each channel of a pulse height analyzer, one can readily measure the cluster size distribution histogram. A more detailed account of this method is given elsewhere.[11,13]

(c) Data Analysis. We are interested in experimentally obtaining the quantity b defined in terms of the number fraction $\sum_1^\infty X_n$ of clusters and the weight fraction $X_0 = \sum_1^\infty nX_n$ in eq 2. These two fractions can be determined quite readily by using the resistive pulse method. Suppose we measure in an unaggregated sample $\mathcal{N}_0$ latex spheres traversing the sensing pore in a fixed time T (generally 200 s). This number $\mathcal{N}_0$ is proportional to the weight fraction X_0 of latex spheres in the sample: $\mathcal{N}_0 = q'X_0$. Here q' is proportional to the rate of flow across the pore. If the aggregation is allowed to take place, clusters will form. Let $\mathcal{N}_n$ be the number of clusters containing n units that pass the pore in counting interval T. We also define as $\mathcal{N}_a$ the total number of clusters, regardless of size, that pass the pore in interval T. Then by definition

$$\mathcal{N}_a \equiv \sum_{n=1}^{\infty} \mathcal{N}_n \tag{3}$$

If, as is the case in our experiments,[10] the clusters are smaller than the pore size and if they remain randomly dispersed despite the influence of gravity, then $\mathcal{N}_n$ will be proportional to the mole fraction X_n of clusters of size n in the reaction mixture. That is, $\mathcal{N}_n = q''X_n$, where q'' is proportional to the rate of flow of the aggregating reaction mixture across the pore. Thus

$$\mathcal{N}_a = q'' \sum_1^\infty X_n \tag{4}$$

Generally the flow rate is unaffected by the aggregation so that $q'' = q'$, and hence

$$\sum_1^\infty X_n / X_0 = \sum_1^\infty \mathcal{N}_n / \mathcal{N}_0 \tag{5}$$

Thus b is determined directly by measuring $\mathcal{N}_a$ and $\mathcal{N}_0$ as

$$b = 1 - \mathcal{N}_a / \mathcal{N}_0 \tag{6}$$

In the regime $b \ll 1$, $\mathcal{N}_a/\mathcal{N}_0 \sim 1$, and any possible small variation in the flow rates q' and q'' can produce an error in the determination of b. Thus for the cases in which $b < 0.2$ we determined both $\mathcal{N}_a$ and $\mathcal{N}_0$ for the *aggregated* sample. By definition $\mathcal{N}_0 = \sum n\mathcal{N}_n$. For small b the $\mathcal{N}_n$ distribution falls off very rapidly with increasing n, so that $\mathcal{N}_0$ can be computed accurately from the experimental histogram. In the regime $b \gtrsim 0.5$, $\mathcal{N}_a/\mathcal{N}_0$ becomes much smaller than unity and henceforth b becomes relatively insensitive to possible small differences in the flow rates q' and q''. Also in this regime the $\mathcal{N}_n$'s fall off rather slowly with n so that $\mathcal{N}_0$ cannot be reliably found from $\sum n\mathcal{N}_n$. Thus in this regime $\mathcal{N}_0$ was determined from the unaggregated sample and $\mathcal{N}_a$ from the aggregated one. As a final consideration which affects the accuracy with which the $\mathcal{N}_n$'s can be determined, we must mention the possibility of coincidences, i.e., two clusters in the pore simultaneously. The electronic detection system of our apparatus senses such a "coincidence" in either of two ways. Either the coincidence is counted as a particle having a mass equal to the sum of the masses of the two particles or the second particle is not detected at all. If V_p is the fluid volume that passes through the pore in the counting time T and if $\bar{V}$ is the average volume available to each particle in the solution, then the probability that n particles occupy the pore during time T is given by the Poisson distribution $P(n) = (V_p/\bar{V})^n e^{-(V_p/\bar{V})}/n!$ We arranged that the ratio $V_p/\bar{V}$ was typically smaller than 0.03. Under these conditions the probability that two or more particles are to be found in the pore during time T is so small that the corresponding error in b due to such coincidences is less than 0.03. In addition, we developed a method to correct for coincidences, which further reduces errors in the determination of b. With this method we find that coincidences affect our determination of b only in the regime $b < 0.1$. Hence the error in b so produced is ~10–20%.

(d) Solution Ionic Strength (I) and pH. In all our experiments the solution pH was 8.15, corresponding to the pK of this buffer solution. Since no other than the buffer concentrations were present in solution, the ionic strength (I) of each solution was equal to half the molarity of the buffer concentration, viz., 0.05 mol/L.

Experimental Results

The form of the cluster size distribution was studied as a function of the time t, the concentration of spheres initially added $[C_0]$, and $[ab]_0$, the concentration of antibodies initially added. It was found that the form of the distribution is determined entirely by the magnitude of the bonding parameter b, regardless of the particular choice of $[C_0]$, $[ab]_0$, and t. The distributions have the form given in eq 1. Different choices for $[C_0]$, $[ab]_0$, and t that produce the same b generate identical cluster size distributions. The present experiments permit us to determine the functional form for $b = b([C_0],[ab]_0,t)$.

In Figure 1 we present a plot of b vs. the time for a series of agglutination reactions for which $[C_0]$ was constant and equal to $3 \times 10^9/\text{cm}^3$ or $[C_0] \cong 0.5 \times 10^{-11}$ mol/L. Each $b(t)$ curve corresponds to a different value of $[ab]_0$. In fact, $[ab]_0$ is in the range $5 \times 10^{-11} \leq [ab]_0 \leq 78 \times 10^{-11}$ mol/L. In this range of $[C_0]$ and $[ab]_0$, b does not exceed ~0.75. Each of the $b(t)$ curves is of the form

$$b(t) = b_\infty F(t) \tag{7a}$$

The detailed form of $F(t)$ is not accurately determined in the data shown in Figure 1. However, over the time domain shown, we can see that $F(t)$ is a monotonic function of t with the following properties.

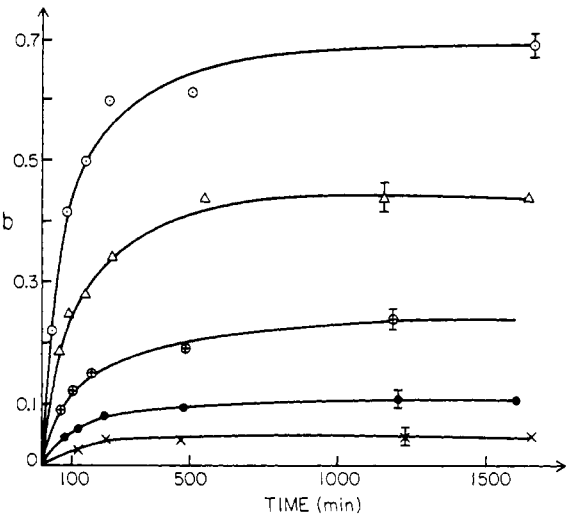

Figure 1. Dependence of b on the time t for a reaction mixture in which $[C_0] = 3 \times 10^9/\text{cm}^3 = 0.5 \times 10^{-11}$ mol/L ($I = 0.05$ mol/L, pH 8.15). The initial antibody concentration, $[ab]_0$, is different for each curve: (⊙) $[ab_0] = 7.8 \times 10^{-10}$, (△) $[ab_0] = 3.9 \times 10^{-10}$, (⊕) $[ab]_0 = 1.95 \times 10^{-10}$, (●) $[ab]_0 = 1.0 \times 10^{-10}$, and (×) $[ab]_0 = 0.5 \times 10^{-10}$ mol/L.

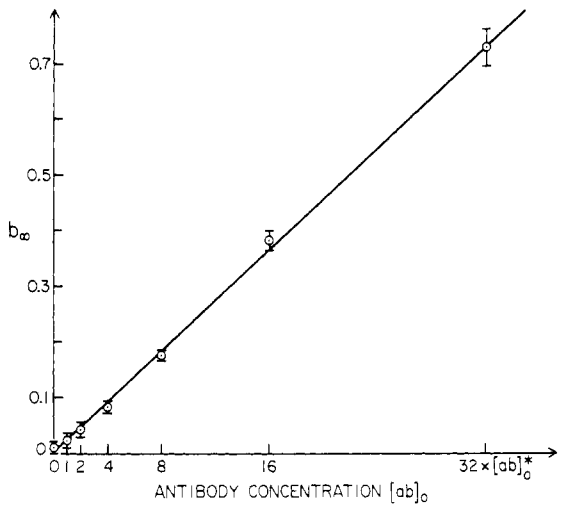

Figure 2. Asymptotic value of b (b_∞) vs. antibody concentration $[ab]_0$ for a reaction mixture in which $[C_0] = 3 \times 10^9/\text{cm}^3$ and $I = 0.05$ mol/L. The quantity $[ab]_0^*$ is equal to 2.44×10^{-11} mol/L.

$$F = \tfrac{1}{2} \quad \text{when } t \cong 100 \text{ min} \equiv \tau_{1/2} \text{ for all } [ab]_0$$
$$F \to 1 \quad \text{for } t \gg \tau_{1/2} \tag{7b}$$
$$F \to 0 \quad \text{for } t \ll \tau_{1/2}$$

The dependence of b_∞ on $[ab]_0$ is shown in Figure 2. Here we plot b_∞ vs. $[ab]_0$ for a series of reactants for which $[C_0] = 3 \times 10^9/\text{cm}^3$, $I = 0.05$ mol/L, and $5 \times 10^{-11} \leq [ab]_0 \leq 78 \times 10^{-11}$ mol/L. Clearly, b_∞ varies linearly with $[ab]_0$ over the range of antibody concentration shown. For larger values of $[ab]_0$, however, b_∞ is no longer linear in $[ab]_0$. Indeed b_∞ shows a maximum as $[ab]_0$ is increased beyond 78×10^{-11} mol/L.

We also investigated the dependence of b on sphere concentration $[C_0]$ for fixed antibody concentration. In Figure 3 we show b vs. $[C_0]$ for two fixed times and for $[ab]_0 = 3 \times 10^{-10}$ mol/L. $I = 0.05$ mol/L. These data show that b is independent of $[C_0]$ for both $t \gg \tau$ and $t \sim \tau$. We conclude that in eq 7 the quantity b_∞ is independent of $[C_0]$. Thus, if we confine ourselves to the regime of $[ab]_0$

Table I
Physical Characterization of the Reaction Mixtures Studied in Figure 1

$[ab]_0$, mol/L	X_0, mol/L	$\bar{e} = [ab]_0/X_0$	b_∞	$b_\infty/\bar{e}$	$\sum_{n=1}^{\infty} X_n(t \to \infty)/X_0$ $Z(t \to \infty)/X_0$
0.5×10^{-10}	0.5×10^{-11}	10	0.04	0.4×10^{-2}	0.96
1.0×10^{-10}	0.5×10^{-11}	20	0.10	0.5×10^{-2}	0.90
1.95×10^{-10}	0.5×10^{-11}	39	0.23	0.59×10^{-2}	0.77
3.9×10^{-10}	0.5×10^{-11}	78	0.43	0.55×10^{-2}	0.57
7.8×10^{-10}	0.5×10^{-11}	156	0.72	0.46×10^{-2}	0.28

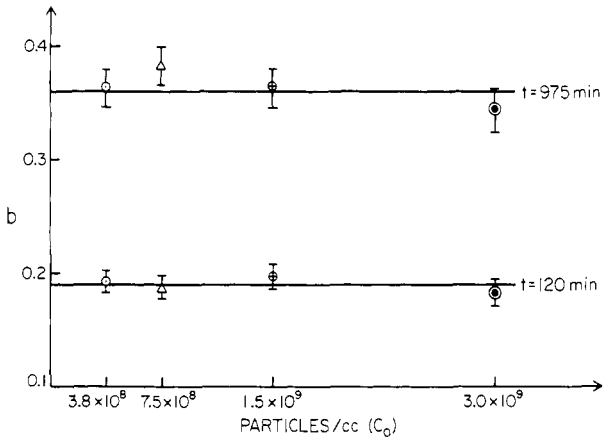

Figure 3. Dependence of b on the concentration of latex spheres for fixed $[ab]_0$ concentration ($[ab]_0 = 3 \times 10^{-10}$ mol/L) for two times: t_2 (long compared to reaction time τ) and t_1 (of the same order as the reaction time $\tau = 90$ min).

concentrations above, we can write $b_\infty = \gamma[ab]_0$, where γ is a constant independent of $[C_0]$. Using the data shown in Figure 2, we deduce that $\gamma = 0.91 \times 10^9$ $(mol/L)^{-1}$. The finding that b is also independent of $[C_0]$ for $t = 120$ min suggests that $\tau_{1/2}$ may also be independent of sphere concentration. We cannot be sure of this from the results in Figure 3 because $F(t)$ becomes rapidly independent of $\tau_{1/2}$ for $t > \tau_{1/2}$.

As mentioned previously, for each fixed value of $[C_0]$, the linear dependence of b_∞ upon $[ab]_0$ applies only over a limited range. Indeed b_∞ reaches a maximum value and then decreases as $[ab]_0$ increases beyond a certain value $[ab]_0^m$, which in turn depends on $[C_0]$. We can obtain considerable insight into the conditions under which the data shown in Figures 1–3 were obtained by considering somewhat more carefully the relationship between $[ab]_0^m$ and $[C_0]$. Here we apply an analysis developed previously for a different system.[14] Consider first the initial prompt binding of the antibody to the antigenic sites on the spheres. If this binding is regarded as reversible and if [agab] is the equilibrium concentration of ag–ab pairs, f the number of antigens per carrier particle, and K_0 the binding constant for the ag–ab bonding, then in accordance with chemical equilibria we may write

$$[agab] = K_0([ab]_0 - [agab])(f[C_0] - [agab]) \quad (8)$$

Since $\bar{e} = [agab]/[C_0]$ is the mean number of singly-bound antibodies per sphere in this first step of antibody binding to spheres, we rewrite eq 8 in the following way:

$$[ab]_0 = [C_0]\bar{e} + \frac{\bar{e}}{f - e}\left(\frac{1}{K_0}\right) \quad (9)$$

In the second stage of the aggregation process the singly-bound bivalent antibodies on the diffusing spheres link to unoccupied antigenic sites on *other* spheres. For this stage we expect that the probability of bonding between individual spheres will be proportional to $\bar{e}(f - \bar{e})$. Thus qualitatively we expect that maximum bonding will occur under conditions in which $\bar{e}(f - \bar{e})$ is maximal. This occurs for $\bar{e} = f/2$. Under these conditions we can expect that b_∞ is maximal.

Using $\bar{e} = f/2$ in eq 9, we obtain the following relationship between $[ab]_0^m$ and $[C_0]$, assuming chemical equilibrium for the binding of antibody to the antigen-coated carrier particles:

$$[ab]_0^m = [C_0]\frac{f}{2} + \frac{1}{K_0} \quad (10)$$

In our system we determined $[ab]_0^m$ and $[C_0]$ and found a straight-line relationship between them over the following range in $[C_0]$: $3.8 \times 10^8/cm^3 < [C_0] < 9.6 \times 10^9/cm^3$. From that data we deduced $f = 2400 \pm 200$. The value of $1/K_0$ is very small; i.e., $1/K_0 \leq 2 \times 10^{-10}$ mol/L. If one uses these values of f and K_0 in eq 9 and applies this equation to the experimental data shown in Figures 1–3, one may draw the following conclusions. First, in all cases the second term in eq 9 can be neglected. That is, $\bar{e} \cong [ab]_0/[C_0]$: essentially all the antibody is bound to the antigenic sites on the spheres. Second, in the case of minimal aggregation, such as that which occurs for the case $b_\infty \simeq 0.04$, corresponding to the lowest of the $b(t)$ curves in Figure 1, $\bar{e} = [ab]_0/[C_0] = 10$. On the other hand, when $b_\infty = 0.72$, corresponding to the most aggregation in Figure 1 or 2, $\bar{e} \cong 160$.

It is quite useful to characterize each of the reaction mixtures studies in Figure 1 in terms of $\bar{e}$ and b_∞. This is done in Table I. In column 1 of this table are listed the initial antibody concentrations $[ab]_0$ for each curve in Figure 1. Column 2 lists the sphere concentration, and column 3 lists $\bar{e}$, the mean number of initially bound antibodies per sphere that are presumably available for subsequent bridge formation between spheres. Column 4 lists b_∞, the mean number of bridge-forming bonds achieved per sphere by the end of the reaction (deduced from the cluster size distributions using eq 2). Column 5 shows that the fraction of initially bound antibodies that actually form bridges between spheres is only about 0.5% for all the reaction mixtures shown in Figure 1. If this fraction is the same for spheres in the interior of a cluster and spheres at the surface, it would appear that the reaction is stopping even though each surface sphere has nearly $\bar{e}$ antibodies still available for further bridge formation with other clusters. The striking fact that the reaction stops under conditions apparently favorable for further reaction will be discussed in the subsequent theoretical section. In column 6 we list the fractional number of clusters $Z/X_0 = \sum_1^\infty X_n(t \gg \tau_{1/2})/X_0$ formed at the end of each of the reactions shown in Figure 1. $Z = \sum_1^\infty X_n$ is the total mole fraction of clusters regardless of size. Column 6 shows that for the various reaction mixtures studied in Figure 1, the total final number of clusters is between 0.96 and 0.28 times the initial number of spheres.

In the reaction mixtures described in Figures 1–3 the antibody and sphere concentrations were such that $\bar{e}$ is

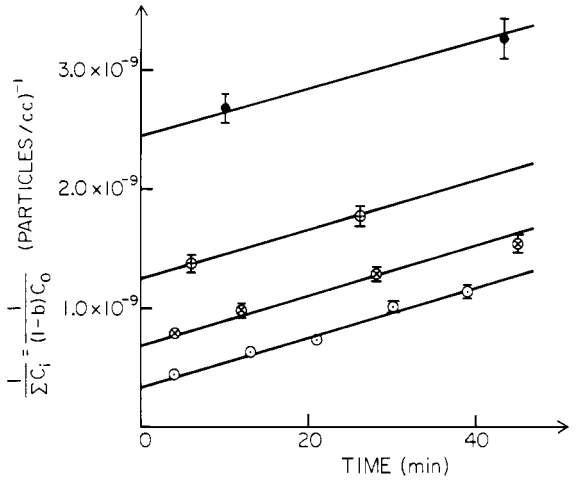

Figure 4. Temporal evolution of the reciprocal of the total number of clusters for short times. In each experiment $[C_0]$ and $[ab]_0$, respectively, have the values $[C_0] = 3 \times 10^9(2^{-y})/cm^3$ and $[ab]_0 = 6.25 \times 10^{-9}(2^{-y})$ mol/L. $y = 0$, 1, 2, and 3, respectively, for the data indicated by ⊙, ⊗, ⊕, and ●.

small compared to f. We also studied, for short times, reaction kinetics under conditions in which the antibody concentration was raised to the level that $[ab]_0 = [ab]_0^m$ for each sphere concentration used. In these experiments we measured the time dependence of the total mole fraction of clusters $\sum X_n(t)$ vs. the time for times smaller than $\tau_{1/2}$. In Figure 4 we plot $1/\sum C_n(t)$ vs. t for various values of $[C_0]$ and the corresponding $[ab]_0^m$. (Note $C_n = X_n/6.02 \times 10^{20}\bar{V}$, where $\bar{V}$ is the molar volume of water in liters/mole.) For each of the four curves $[C_0] = 3 \times 10^9(2^{-y})/cm^3$ and $[ab]_0 = 6.25 \times 10^{-9}(2^{-y})$ mol/L, with $y = 0$–3. Thus the ratio $[ab]_0/[C_0]$ is the same for all the mixtures. We observe that over the time domain studied, the plots of $1/\sum C_n(t)$ are linear in t and all have the same slope of 2.1×10^{-11} cm³/min = 1.26×10^{10} L/(mol min) independent of $[C_0]$. According to the definition of b

$$1/\sum_1^\infty C_n(t) = 1/[C_0](1 - b) \tag{11a}$$

Thus

$$\frac{d}{dt}(1/\sum_1^\infty C_n(t)) = \left(\frac{db}{dt}\right)(1/[C_0](1 - b)^2)$$

which, in the limit $b \ll 1$ becomes

$$\frac{d}{dt}(1/\sum_1^\infty C_n(t)) \cong \frac{1}{[C_0]}\frac{db}{dt} \qquad b \ll 1 \tag{11b}$$

We also examined the possible reversibility of the aggregation process in the following manner. We added a great excess of antibody. The concentration was ~1 g/mol ≃ 1.6×10^{-5} mol/L. This is about 3 orders of magnitude greater than the concentration of all the antigenic sites $f[C_0] \sim 1.2 \times 10^{-8}$ mol/L. Under conditions of thermodynamic equilibrium, bridge formation and breakup would be occurring. Any broken bridge would be replaced by two singly-bonded antibodies under the conditions of high antibody concentration, and consequently in time the clusters would break up. When the saturation experiment was performed on systems in which b had reached its steady-state value, there was no observed break up of clusters whatever even though the reactions were studied over a period of 48 h, a time very long compared to the time constant $\tau_{1/2}$. For reactions in which $db/dt \neq 0$ the addition of excess antibody immediately stopped the progress of the reaction, presumably by binding to all the antigenic sites and preventing any further double-bond formation. In these systems as well no subsequent break up of double bonds was observed over an observation period of 48 h. We must conclude from these observations that the process of cross-linking between spheres is irreversible in our system.

Theoretical Discussion

We have not found in the extant literature a theory capable of fully explaining both the observed form of the cluster size distributions (eq 1) and the observed dependence of b upon $[ab]_0$, $[C_0]$, and the time t.

If we apply the Flory–Stockmayer statistical analysis[2,8] to our RA_f–B_2 system, the distribution that is predicted has the form[15,16]

$$\frac{X_n}{X_0} = \frac{e^{-2nb}(2nb)^{n-1}}{nn!} \tag{12}$$

This theoretical form, is distinctly different from that found experimentally. Moreover, it predicts a sol–gel transition at $b = {}^1/_2$, a phenomenon that does not occur in our system. We believe that such a statistical analysis[2,8] is appropriate for distributions that are in thermal equilibrium.[9] In the present case the experiments described above clearly indicate that our system is evolving under unidirectional kinetic control. We therefore take the unidirectional Smoluchowski equations[1-7] as the starting point of our analysis, viz.

$$\frac{dX_n}{dt} = \frac{1}{2}\sum_{n'=1}^{n-1} a_{n-n',n'}X_{n-n'}X_{n'} - \sum_{n'=1}^{\infty} a_{nn'}X_nX_{n'} \tag{13}$$

The form of the solutions of these equations is determined by the dependence of the bimolecular reaction rate coefficients $a_{nn'}$ upon n and n'. In principle we need a microscopic theory for this bimolecular reaction rate coefficient: a theory that takes into account the fact that after the prompt binding of antibodies, each sphere has a Poisson distribution of antibodies potentially available for bridge-forming bonds. In the absence of a microscopic theory appropriate for our system of slowly diffusing spheres, each having a distribution of reactive sites, we proceed in a heuristic fashion to search for a structure of the $a_{nn'}$ that is consistent with our experimental findings. Taking this point of view, we have observed previously[9,10,12] that if $a_{nn'} = B(n + n')$, then the predicted cluster size distributions have the same dependence upon b and n as is found experimentally.

Using this form for $a_{nn'}$, we can use the Smoluchowski equations to obtain the time dependence of b. Indeed inserting $a_{nn'} = B(n + n')$ into eq 13 and summing over all n, we obtain the following equation[17] for $b(t)$:

$$db/dt = B(1 - b)[C_0] \tag{14}$$

According to this equation, if B is independent of the time, b asymptotically always approaches unity with a time constant $\tau = 1/B[C_0]$. Our experimental data show, however, that the final steady-state value of b is not unity but is a quantity proportional to $[ab]_0$ and independent of $[C_0]$. Moreover, the data in Figure 3, while not conclusive, suggest that the reaction time $\tau_{1/2}$ found experimentally may be independent of $[C_0]$.

To account for these effects we propose to consider more carefully the implicit assumption that B is a constant. Physically B is a measure of the probability that a single sphere on one cluster will react with another sphere on a different cluster. Thus we can expect crudely that

$$B = \beta\bar{e}\bar{g} \tag{15}$$

Here $\bar{e}$ is the mean number of singly-bound antibodies on

a sphere, and $\bar{g}$ is the mean number of complementary unbound antigenic sites on another reacting sphere. β is assumed to be a constant of proportionality. If B is independent of the time, the final steady-state value of b is always unity. The equation for $b(t)$ can produce asymptotic values for $b(t \to \infty)$ less than unity provided that B is time dependent. This can occur if the average number $\bar{e}$ of potential bridge-forming antibodies decreases with the time. There is, in fact, a possible mechanism for this inactivation process: namely, the binding of the second arm of the antibody to another antigen on the surface of its own sphere. Indeed the mean separation l of antigens on the surface of each sphere of radius R_0 containing f antigens is $l \cong R_0/(f/4\pi)^{1/2}$. Since our spheres have $R_0 \cong$ 1170 Å and $f = 2400$, it follows that $l \sim 80$ Å. This spacing is quite comparable to separation ($\sim$100 Å) between the active sites on the arms of our bivalent antibody. Thus, it is possible that, following the binding of one arm, the second arm subsequently binds to the same sphere with a characteristic time constant τ_A, thereby producing an inactivation of the potential bridge-forming antibodies. According to this mechanism, we may model the time dependence of $\bar{e}$ as

$$\bar{e}(t) = \bar{e}_0 e^{-t/\tau_A} \tag{16a}$$

Here

$$\bar{e}_0 = [ab]_0/[C_0] \tag{16b}$$

is the mean number of antibodies initially singly bound to each sphere. In effect this proposed mechanism is designed to explain why the reaction stops: the number of bridge-forming antibodies does not remain fixed at its initial value of $[ab]_0/[C_0]$ but decays with a time constant τ_A independent of both the sphere and antibody concentration.

According to this model, the quantity $\bar{g}$ in eq 15 can be related to $\bar{e}$ as follows. Since $\bar{e}_0 - \bar{e}(t)$ is the number of antibodies that connect to two antigenic sites on a single sphere, the mean number $\bar{g}$ of antigenic sites available for cross-linking is $\bar{g} = f - \bar{e} - 2(\bar{e}_0 - \bar{e}(t))$. Thus

$$\bar{g} = f - 2\bar{e}_0 + \bar{e}(t) \tag{16c}$$

In the absence of this inactivation mechanism, $\bar{g} = f - \bar{e}_0$.

We now examine the consequences of this model for the structure of $B(t)$ in the two experimental regimes studied above: case 1, $\bar{e} \ll f$; and case 2, $\bar{e} \sim f/2$.

Case 1: When $\bar{e} \ll f$, we find using eq 15 and 16a–c that eq 14 take the form

$$\frac{db}{dt} \cong \left(\frac{1}{\tau_R}\right) e^{-t/\tau_A}(1 - b) \tag{17a}$$

where

$$1/\tau_R \equiv \beta f [ab]_0 \tag{17b}$$

The solution of (17a) under the initial condition $b(t \to 0) = 0$ is

$$b(t) = 1 - \exp[(-\tau_A/\tau_R)(1 - e^{-t/\tau_A})] \tag{18}$$

According to this equation, when $t \gg \tau_A$, b approaches the asymptotic value b_∞ given by

$$b_\infty = 1 - e^{-\tau_A/\tau_R} \tag{19}$$

Observe that for $b_\infty \ll 1$, i.e., $\tau_A/\tau_R \ll 1$, $b_\infty \cong \tau_A/\tau_R$. Thus we have the following expression for b_∞ in terms of the two theoretical parameters β and τ_A:

$$b_\infty \cong \beta f \tau_A [ab]_0 \qquad b_\infty \ll 1 \tag{20}$$

We can obtain a second independent equation for β and τ_A by considering the initial slope of the $b(t)$ curves. Again if $b_\infty \ll 1$, and $t/\tau_A \ll 1$, eq 18 reduces to the form $b(t) \cong t/\tau_R$; thus we have

$$db/dt \cong \beta f [ab]_0 \tag{21}$$

for $\tau_A/\tau_R \ll 1$, $t/\tau_A \ll 1$. From experimental measurements of both b_∞ and db/dt in the limits indicated, the data should permit the separate determination of β and τ_A.

We may now compare our theory to the experimental results found previously to check the predicted functional form for b_∞ and $(db/dt)_{t\to 0}$ and to deduce the numerical values of the two parameters β and τ_A. By estimating the initial slope of the data shown in Figure 1, we find approximately that

$$\frac{1}{[ab]_0}\left(\frac{db}{dt}\right) \cong 10 \times 10^6 \text{ L/(mol min)} \tag{22}$$

for $t/\tau_A \ll 1$ and $b_\infty \ll 1$. According to the theoretical result, eq 21, the quantity on the right-hand side of eq 22 is equal to the constant βf. Using $f = 2400$, we deduce the numerical value of β as

$$\beta \cong 4.2 \times 10^3 \text{ L/(mol min)} \tag{23}$$

Turning now to the experimental values of b_∞, we observe that $b_\infty = \gamma[ab]_0$, where $\gamma = 0.91 \times 10^9$ L/mol. This finding is in agreement with the predicted form in eq 20. Indeed according to this equation

$$\gamma = \beta f \tau_A$$

Since $\beta f = (1/[ab]_0)(db/dt)_{t\to 0}$ from eq 21, we can obtain τ_A numerically as

$$\tau_A = \gamma/[(1/[ab]_0)(db/dt)_{t\to 0}] \tag{24a}$$

or

$$\tau_A = [0.91 \times 10^9 \text{ L/mol}]/[10 \times 10^6 \text{ L/(mol min)}]$$

Thus

$$\tau_A \cong 90 \text{ min} \tag{24b}$$

We now turn to an analysis of our findings for $b(t)$ in the regime in which $\bar{e}_0$ is not small compared to f, i.e., case 2 above. (Notice that the number of antibodies initially bound to each sphere cannot exceed f.) We can solve eq 14 using eq 15 and 16a–c, for arbitrary $0 \le \bar{e}_0 \le f$, to obtain the following general result for the time dependence of b:

$$1 - b(t) = \exp\left[-\beta[C_0]\tau_A\bar{e}_0\left\{(f - 2\bar{e}_0)(1 - e^{-t/\tau_A}) + \frac{\bar{e}_0}{2}(1 - e^{-2t/\tau_A})\right\}\right] \tag{25}$$

From this result it follows that b_∞ is

$$b_\infty = 1 - \exp[-\beta[C_0]\tau_A\bar{e}_0\{f - \tfrac{3}{2}\bar{e}_0\}] \tag{26}$$

Thus, this kinetic analysis implies that b_∞ varies linearly with $[ab]_0$ provided that $\bar{e}_0 \ll f$. Upon increasing $\bar{e}_0$, however, b_∞ takes on a maximum value and then decreases because of the factor $\bar{e}_0\{f - (3/2)\bar{e}_0\}$. Indeed, according to this kinetic analysis, b_∞ takes on its maximum value when $\bar{e}_0 \equiv \bar{e}_0^m = f/3$. It will be noted that the equilibrium analysis as discussed above predicts that b_∞ will be maximized when $\bar{e} = f/2$. Thus, according to the unidirectional kinetic theory, it is possible that $f = 3600$ for our system. Despite this possibility, for the purposes of discussion, we shall retain the value $f = 2400$ estimated from our data using the equilibrium theory (eq 10).

For short times, as was the case for the data in Figure 4, $b(t)$ is linear in t and according to eq 25, $b(t)$ has the form

$$b(t) = \beta[C_0]\bar{e}_0(f - \bar{e}_0)t \quad (27a)$$

The data in Figure 4 were obtained for values of the antibody concentration that maximized b_∞. This implies $\bar{e}_0 = f/3$ for this kinetically controlled system. Using this value of $\bar{e}_0$ in eq 27a gives

$$b(t) = (2/9)\beta f^2[C_0]t \quad (27b)$$

We now compare this prediction with the experimental findings of Figure 4. First we observe that for the earliest times shown in the figure, i.e., ~4–5 min, b is not negligibly small but is in fact about 0.175. Thus it is difficult to assess accurately db/dt in the limit $b \to 0$. We can proceed crudely by using the $t = 0$ intercept for $1/[C_0]$ and the first point at $t \sim 4$–5 min. According to this and using eq 11a, we find that $(1/[C_0])(db/dt) = (1 - b)^2[d(1/\sum C_n(t))/dt] \cong (0.825)^2(1.26 \times 10^{-10}) \simeq 0.85 \times 10^{-10}$ L/(mol min). With this crude estimate for $1/[C_0](db/dt)$ we can estimate β using eq 27

$$\frac{1}{[C_0]}\left(\frac{db}{dt}\right) = \frac{2}{9}\beta f^2 \cong 0.85 \times 10^{-10}\ \frac{\text{L}}{\text{mol min}} \quad (28)$$

With $f = 2400$ we deduce

$$b \cong 6.6 \times 10^3\ \text{L/(mol min)} \quad (29)$$

This value for β is in rough agreement with the value previously deduced in eq 23 from experimental data shown in Figure 1 for the case $\bar{e}_0 \ll f$. In view of the crudeness of the experimental value for $(1/[C_0])(db/dt)$, it clearly is desirable to obtain more accurate data for $b(t)$ under the conditions $\bar{e}_0 = \bar{e}_0^m$.

Conclusions

We have shown[10] that the cluster size distributions for our system of high-functionality antigens cross-linked by antibody have the form given by eq 1. The dependence of the distributions on the time t, antibody concentration $[ab]_0$, and sphere concentration $[C_0]$ are contained in the bonding parameter b. We have presented above the experimentally observed functional form for $b([ab]_0,[C_0],t)$. In order to understand both the structure of the distributions and the functional form for b, we have employed the unidirectional Smoluchowski kinetic equations, whose solutions provide both the structure of the cluster size distributions and the temporal evolution of the bonding parameter b in terms of the form of the bimolecular reaction coefficient $a_{nn'}$. In the absence of a microscopic theory for this coefficient, we have proposed on purely phenomenological grounds that $a_{nn'}$ has the following form in our system:

$$a_{nn'} = \beta\bar{e}\bar{g}(n + n') \quad (30a)$$

where $\bar{e}$, the mean number of potential bridge-forming antibodies bound to each sphere, decays in time according to

$$\bar{e} = \bar{e}_0 e^{-t/\tau_A} \quad (30b)$$

and $\bar{g}$ is the number of complementary antigenic sites on each sphere. With eq 30 it has proven possible to make predictions for both the form of the distributions and the functional dependence of b on t, $[ab]_0$, and $[C_0]$ that are in substantial agreement with the experimental findings reported here.

It remains to be seen how one can justify on a microscopic level the assumed structure for $a_{nn'}$ (eq 30a). The dependence on n and n' in the form $n + n'$ is known to be valid for monomers of the form BRA_{f-1}, with only A–B bonds allowed. However, in our system the monomer units have a very different form, being of the B_eRA_{f-e} type. Here e is a random variable distributed according to Poisson statistics around a value $\bar{e}$, which in our experiments is in the range 10–150 and was also as large as 1200. It is by no means clear how such a system of monomer units can produce a bimolecular reaction rate coefficient that varies with n, n', and $\bar{e}$ as proposed in eq 30a.

Second we need some independent binding experiments to more directly investigate our assumptions that the bridge-forming antibodies are becoming inactivated in time in accordance with eq 30b.

Finally, it is important to test much more accurately than is possible with the present data the precise temporal evolution of b over a wider range of the parameters $[ab]_0$ and $[C_0]$.

Acknowledgment. This work was supported in part by contract No. N00014-80C0500 from the Office of Naval Research, by the National Science Foundation under grant No. PCM8013659, and by the Center for Materials Sciences and Engineering, MIT, under National Science Foundation Grant No. 78-24185 DMR. We are grateful to Dr. Hans Hager of the Hoffmann-La Roche Co., Nutley, NJ, for providing the hSA-coated spheres and the anti-hSA antibody. G.K.v.S. is grateful to the following institutions for support during various stages of this work: The Whitaker Health Sciences fund at MIT, the Steo Stiftung of Zurich, the Geigy Jubilaums-Stiftung of Basel, and the Swiss National Science Foundation. G.B. acknowledges with gratitude the hospitality of the Department of Physics at the University of California at Santa Barbara, where the manuscript was written.

References and Notes

(1) von Smoluchowski, M. *Phys. Z.* **1916**, *17*, 585. *Z. Phys. Chem.* **1917**, *92*, 129.
(2) Stockmayer, W. H. *J. Chem. Phys.* **1943**, *11*, 45; **1944**, *12*, 125.
(3) Golovin, A. H. *Izv. Geophys. Ser.* **1963**, *5*, 482.
(4) McCleod, J. B. *Q. J. Math. Oxford* **1962**, *13*, 119, 193, 283.
(5) Lushnikov, A. A. *J. Colloid Interface Sci.* **1978**, *65*, 2, 276.
(6) Ziff, R. M. *J. Stat. Phys.* **1980**, *23*, 241.
(7) Ziff, R. M.; Stell, G. *J. Chem. Phys.* **1980**, *73*, 3492.
(8) Flory, P. J. "Principles of Polymer Chemistry"; Cornell University Press: Ithaca (NY) and London, 1953.
(9) Cohen, R. J.; Benedek, G. B. *J. Phys. Chem.* **1982**, *86*, 3696.
(10) von Schulthess, G. K.; Benedek, G. B.; De Blois, R. W. *Macromolecules* **1980**, *13*, 939.
(11) De Blois, R. W.; Bean, C. P. *Rev. Sci. Instrum.* **1970**, *41*, 909.
(12) von Schulthess, G. K. Ph.D. Thesis, MIT, 1979. (A limited number of copies of this thesis are available on request.)
(13) De Blois, R. W.; Bean, C. P.; Wesley, R. *J. Colloid Interface Sci.* **1977**, *61*, 2, 323.
(14) von Schulthess, G. K.; Cohen, R.; Sakato, N.; Benedek, G. *Immunochemistry* **1976**, *13*, 955.
(15) Calvert, P. D.; Nichol, L. W.; Sawyer, W. H. *J. Theor. Biol.* **1979**, *80*, 233.
(16) Goldberg, R. W. *J. Am. Chem. Soc.* **1952**, *74*, 5715.
(17) In eq 13 we use X_n to denote the concentration of clusters of size n in units of mole fraction, X_0 being the concentration of spheres initially added in mole fraction units. In eq 14, to facilitate comparison with experimental data we express X_0 not in mole fraction units but in units of moles/liter and use $[C_0]$ to denote X_0 in these units.